from 304 to 311, where partially deuterated products would be seen, only the 310 (M - D) peak had intensity >1%.

The **X-ray structure** was determined on an Enraf-Nonius CAD4 diffractometer. The triclinic cell parameters are given in Table I; the structure was refined in space group $P\bar{1}$ (No. 2). Details of the X-ray analysis are given in the supplementary material.

***t* tests** were performed using the InStat program from GraphPAD Software, Inc.

AM1 calculations[22] were performed on a MicroVAX computer using the MOPAC suite of programs.[23]

Acknowledgment. This work was supported in part by the National Science Foundation through Grant No. RII-8902064, the State of Mississippi, and the University of Mississippi.

Supplementary Material Available: Crystallographic data for **4**, including experimental procedures, atomic coordinates, bond lengths, bond angles, torsion angles, and least-squares planes (14 pages). Ordering information is given on any current masthead page.

(22) Dewar, M. J. S.; Zoebisch, E. G.; Healy, E. F.; Stewart, J. P. *J. Am. Chem. Soc.* **1985**, *107*, 3902.

(23) Stewart, J. J. P. *MOPAC A Semi-Empirical Molecular Orbital Program. QPCE* **1983**, 455.

Theoretical Investigation of the Rotational Barrier in Allyl and 1,1,3,3-Tetramethylallyl Ions

James B. Foresman,[†] Ming Wah Wong,[†,‡] Kenneth B. Wiberg,*[,†] and Michael J. Frisch[§]

Contribution from the Department of Chemistry, Yale University, New Haven, Connecticut 06511, and Lorentzian Inc., North Haven, Connecticut 06473. *Received June 29, 1992. Revised Manuscript Received December 22, 1992*

Abstract: Optimized equilibrium geometries and rotational transition structures for allyl and methyl-substituted allyl ions are obtained by using Hartree-Fock (HF) and second-order Møller-Plesset perturbation (MP2) theory. For the parent allyl cation, gas-phase stationary points are also found using the quadratic configuration interaction (QCISD) method. At the levels of theory beyond HF, the lowest energy path for exchange of two hydrogens on one terminal carbon in allyl cation is predicted to involve migration of the central hydrogen to the terminal carbon, whereas the anion transforms via the usual perpendicular transition structure. Allyl cation energies are also computed using the highly accurate CCSD(T) and QCISD(T) methods at the MP2 stationary points. Methyl substitution at the terminal carbon which is involved in the rotation stabilizes the perpendicular structure for the cation, and all levels of theory predict the usual transition structure. Finally, solvation effects on the rotational barrier are investigated using an Onsager reaction field model. The gas-phase rotational barriers of 19.4 and 8.6 kcal/mol calculated for the tetramethylallyl cation and anion, respectively, are reduced to 17.8 and 7.0 in a medium of dielectric constant 78.5.

Introduction

Charge-delocalized carbocations such as allyl cations and nonclassical carbocations have received considerable attention. Allyl cations are of importance because they are involved in a variety of chemical[1] and biochemical processes.[2] Many cations such as the ethyl cation adopt bridged structures, at least in the gas phase.[3] Charge delocalization provides two energetic benefits. First, if electrons flow toward an empty p orbital, a region of low potential energy for an electron, the total energy of the ion will be decreased. Second, in the gas phase, spreading the charge over as large a volume as possible will reduce the electrostatic energy of the ion and make it more stable. Solvents will not affect the first of these terms, but a polar solvent will markedly reduce the importance of the electrostatic energy. As a result, the advantage of bridging will be decreased in the presence of such solvents. Thus, we have begun a series of investigations of the effect of solvents on the properties of charge-delocalized cations.

This report will be concerned with the simplest of these ions, the allyl cation. The barrier to rotation has been used as a measure of the "resonance energy".[4] However, as we have noted, the barrier will arise from both of the terms noted above.[5] A 90° rotation of one methylene group will eliminate the interaction of the π-bond with the cationic p orbital and at the same time will restrict the charge to a smaller volume element, resulting in an increase in the electrostatic energy. We will examine the rotational barrier, the effect of methyl substitution, and the effect of polar solvents. We shall also examine the related allyl anion in order to gain information on the difference between charge-delocalized carbocations and anions. Some difference would be expected since the anions do not have a bonding orbital into which the π-electrons may be delocalized.

There have been many experimental[6] and theoretical[4,5,7] attempts to understand the structure and energetics of rotational isomerism in these ions. There remains some uncertainty regarding the general process:

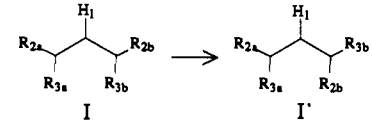

I I'

[†] Yale University.

[‡] Present address: Department of Chemistry, University of Queensland, St. Lucia, QLD 4072, Australia.

[§] Lorentzian Inc.

(1) For a review, see: Deno, N. C. In *Carbonium Ions*; Olah, G. A., Schleyer, P. v. R., Eds.; Wiley: New York, 1970; pp 783-806.

(2) Stryer, L. *Biochemistry*, Freeman: New York, 1988; pp 556-558.

(3) Hehre, W. J.; Radom, L.; Schleyer, P. v. R.; Pople, J. A. *Ab Initio Molecular Orbital Theory*; Wiley: New York, 1986; pp 384-386.

(4) Mayr, H.; Förner, W.; Schleyer, P. v. R. *J. Am. Chem. Soc.* **1979**, *101*, 6032.

(5) Wiberg, K. B.; Breneman, C. M.; LePage, T. J. *J. Am. Chem. Soc.* **1990**, *112*, 61.

(6) (a) Olah, G. A.; Comisarow, M. B. *J. Am. Chem. Soc.* **1964**, *86*, 5682. (b) Schleyer, P. v. R.; Su, T. M.; Saunders, M.; Rosenfeld, J. C. *J. Am. Chem. Soc.* **1969**, *91*, 5174. (c) Deno, N. C.; Haddon, R. C.; Novak, E. N. *J. Am. Chem. Soc.* **1970**, *92*, 6991.

(7) (a) Raghavachari, K.; Whiteside, R. A.; Pople, J. A.; Schleyer, P. v. R. *J. Am. Chem. Soc.* **1981**, *103*, 5649. (b) Cournoyer, M. E.; Jorgensen, W. L. *J. Am. Chem. Soc.* **1984**, *106*, 5104.

0002-7863/93/1515-2220$04.00/0

Table I. Allyl Cation Energies (au) Using the Geometries Optimized at Each Level

structure	RHF 6-31G(D)	RHF 6-311++G(D,P)	MP2-FU 6-31G(D)	MP2-FU 6-311++G(D,P)	QCISD-FU 6-31G(D)
I	-116.193 213	-116.221 592	-116.557 625	-116.669 318	-116.592 716
II	-116.138 989	-116.168 952			
III	-116.132 165	-116.164 582	-116.503 166	-116.619 917	-116.541 674
IV	-116.166 650	-116.196 909	-116.536 121	-116.649 788	-116.575 912
V	-116.166 409	-116.196 567	-116.535 790	-116.649 311	-116.575 651

What is the activation energy? What is the mechanism for the transformation? For R = H, the species in question are too transient to yield accurate experimental data, but ab initio geometry optimizations at the HF/6-31G(D) level (reported in ref 5) have suggested a perpendicular C_s structure for the rotational transition state,

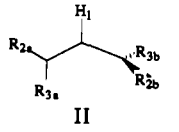

II

In that study, the rotational barrier was calculated at the MP4 level using a very large basis set and the HF/6-31G(D) structures, obtaining 36 and 19 kcal/mol for the cation and anion, respectively. Experimental investigations have been reported only for the 1,1,3,3-tetramethylallyl cation. An analysis of the NMR spectrum for that system in HO_3SF has led to a result in the range of 15–18 kcal/mol[6c] for the rotational barrier. Any theoretical treatment which attempts to account for this number must in some way include the effects of solvent, since experimental conditions within the NMR probe presumably include nontrivial medium effects.[8]

Previous authors have suggested other paths by which isomerization can occur. Consider the following scheme (referred to as path d in ref 6c):

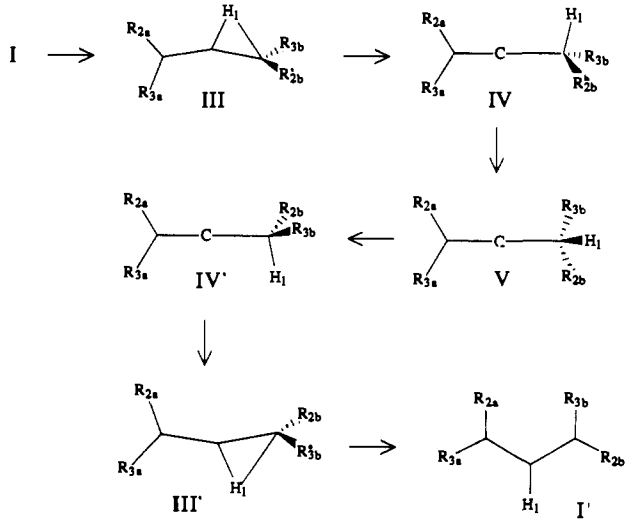

Notice that here the R_{2a} and R_{3a} groups have interchanged, as opposed to the R_{3b} and R_{2b} groups. Another qualitative difference between this path and the one involving a single perpendicular structure is that the formal charge would remain on the central carbon instead of migrating to the carbon whose substituents are interchanging. The authors of ref 6c eliminated this path from consideration on the basis of the relative rates of H–D exchange and methyl interchange in the tetramethyl case. Their final analysis supports a perpendicular rotational transition structure such as II. It is impossible, however, to infer from this what the actual nature of the isomerization process is in the parent cation.

(8) An empirical attempt to account for these solvation effects can be found in ref 4. A more detailed study making use of statistical mechanical Monte Carlo simulations was given in ref 7b. However, in both cases the assumed structure of the transition state has now been found to be incorrect.

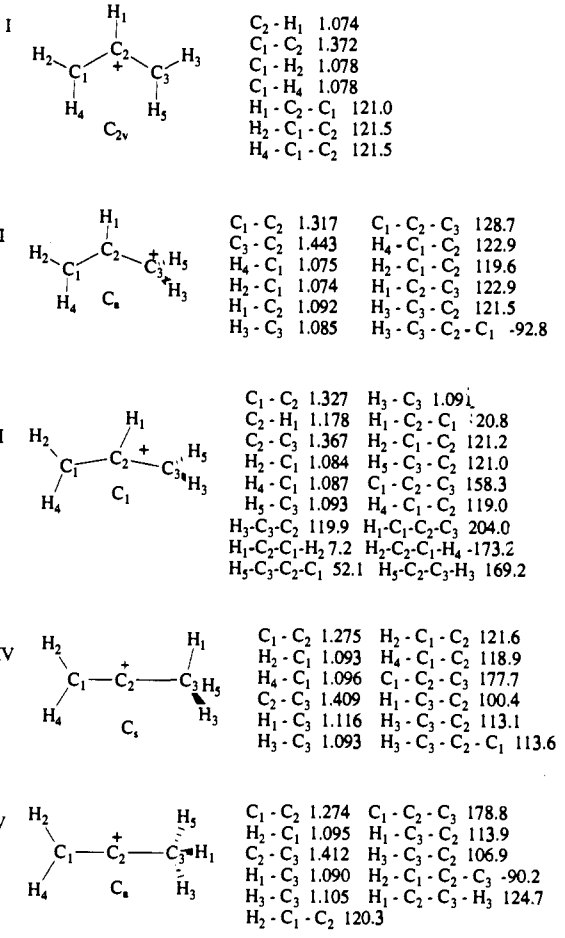

Figure 1. Allyl cation structures. For I the RHF/6-311++G(D,P) structure is given first followed by the MP2/6-311++G(D,P) structure in parentheses. For II only the RHF structure is available. The remaining data were obtained at the MP2/6-311++G(D,P) level of theory.

In this report, we will try to improve the theoretical description of the effects of both methylation and subsequent solvation on the structures and energies of allyl ions. In particular, we would like to assess the need to include electron correlation and solvation effects in the determination of optimized geometric structures and rotational barriers. We also tabulate atomic charges using a variety of established techniques in order to compare their relative utility in rationalizing trends in the energetic results. Finally, a reaction field model[9] based on a spherical cavity has been used to optimize both the equilibrium and rotational transition structures of allyl anion, 1,1,3,3-tetramethylallyl cation, and 1,1,3,3-tetramethylallyl anion in a medium of dielectric constant of 78.5. We chose a dielectric constant near to that of water as our best estimate of the experimental conditions reported in ref 6c.

Allyl Cation

We begin by examining the effect of basis set and electron correlation on type I structures and the energies of allyl cation. Table I contains all energetic results for the levels of theory considered. Figure 1 shows the geometry of I at the RHF/6-

(9) Wong, M. W.; Frisch, M. J.; Wiberg, K. B. *J. Am. Chem. Soc.* **1991**, *113*, 4776.

Table II. Allyl Cation: Relative Total Energies[a] (kcal/mol) of Various Stationary Points

	I	II	III	IV	V
RHF/6-31G(D)	0.0	32.1	35.3	14.1	14.0
RHF/6-311++G(D,P)	0.0	31.1	32.8	12.9	12.9
MP2-FU/6-31G(D)	0.0		31.2	10.9	10.9
QCISD-FU/6-31G(D)	0.0		29.1	7.9	7.9
MP2-FU/6-311++G(D,P)[b]	0.0		28.0	9.7	9.8
CCSD-FC/6-311++G(D,P)	0.0		27.2	8.2	8.3
QCISD-FC/6-311++G(D,P)	0.0		27.1	8.0	8.1
CCSD(T)-FC/6-311++G(D,P)	0.0		26.9	8.9	9.0
QCISD(T)-FC/6-311++G(D,P)	0.0		26.9	8.8	8.8

[a] Includes zero-point vibrational energies (see text). [b] This and the four subsequent calculations utilize the MP2-FU/6-311++G(D,P) structures.

311++G(D,P) level. The MP2[10] and QCISD[11] computations include correlation effects from all electrons. Throughout the article, we will use FU to denote the fact that all electrons have been correlated, while FC will denote the fact that the core orbitals have been deleted. For the most part, geometries are quite insensitive to increasing the basis set beyond 6-31G(D). Correlation effects are small and are adequately included at the MP2 level. Dipole moments and energies are more sensitive to electron correlation. A search for the first-order saddle point corresponding to structure type II was also attempted using each of these theories.

Energies are presented in Table I. Figure 1 contains the RHF/6-311++G(D,P) optimized structure for II. Again, increasing the basis set beyond 6-31G(D) has little effect on geometric parameters, zero-point energies, and dipole moment at the HF level. More interesting is the fact that a similar stationary point could not be found using MP2 and QCISD theories. In each case, optimization proceeds to a C_s minimum (not saddle point) in which the hydrogen of the central carbon has migrated to the terminal carbon (the one whose hydrogens are out-of-plane). The energy of this unusual structure is predicted to be approximately 10 kcal/mol above that of the equilibrium structure. This suggests that there is another route for isomerization which involves three steps: an initial proton shift followed by a methyl rotation and subsequent proton shift back.

The three new types of stationary points discussed in the Introduction need to be considered. Table I contains results for these additional stationary points, while Figure 1 contains the MP2-FU/6-311++G(D,P) optimized structures for each. Structures I and IV are minima while III and V are first-order saddle points (confirmed by evaluating the Hessian for each reported structure). Table II summarizes the relative energies for these structures at various levels of theory. Here the RHF/6-31G(D) zero-point vibrational energies, computed at the RHF/6-31G(D) optimized geometries and scaled by 1/1.12,[12] have been included. For structures I–V these are 41.2, 39.3, 38.2, 38.5, and 38.4 kcal/mol. In HF theory, the path through structure III is higher in energy than the one involving structure II. This is still the case at the larger basis set. It appears, however, that structure II is a "phantom" saddle point and not representative of the true isomerization process. To ensure that the MP2 result is not just an artifact of a second-order correlation treatment, we have also used the more accurate QCISD model with a 6-31G(D) basis to explore the potential energy surface. It too fails to find a stationary point corresponding to structure II and finds structures III, IV, and V, which are similar to the MP2 results. Since structural optimization beyond the MP2 level produces only slight refinement, we decided to use the MP2/6-311++G(D,P) structures and this large basis set to compute the rotational barrier at the QCISD and CCSD[13] levels with and without corrections[14] for triply excited determinants in order to determine how well the results have converged with respect to the inclusion of electron correlation energy. These are also listed in Table II and represent the most sophisticated theoretical parameters for isomerization in allyl cation presented to date. In this case, the CCSD and QCISD results appear to be equivalent, and the barrier to proton migration appears to have converged at approximately 27 kcal/mol.

The real discrepancy between HF and correlated treatments in this case could be traced to the underestimation at HF of the barrier to localize positive charge on a terminal carbon. The resistance to forming a C_s perpendicular structure is seen in the geometric parameters of III. The major structural difference is the deviation from a C_s structure as indicated by the values of the dihedral angles. The theories which include higher electron correlation effects suggest that, as one methylene group twists out of the plane from the equilibrium allyl cation geometry, there is a concomitant decrease of the H_1–C_2–C_3 angle and twisting of the H_1–C_2–C_1–H_2 angle necessary to stabilize the migration of the positive charge.

The mode of "rotation" described above is clearly a means to avoid proceeding through a primary carbocation. These ions are known to have relatively high energies, and the ethyl cation has a hydrogen-bridged structure.[3] The rotational process corresponds to the formation of such a bridged ion as a transition state. It should be possible to minimize the need for such a mechanism by the introduction of methyl groups that will stabilize localized carbocations, and such ions will be considered in a later section of this report.

Table III. Allyl Anion Energies (au) Using the Geometries Optimized at Each Level

	RHF 6-31G(D)	RHF 6-31+G(D)	MP2-FU 6-31+G(D)	RHF-RF[a] 6-31+G(D)
VI	−116.393491	−116.425201	−116.841864	−116.425418
VII	−116.360943	−116.391364	−116.807810	−116.398371

[a] Reaction field with dielectric constant 78.5 and cavity radius 3.6 Å.

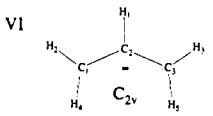

C_2 - H_1 1.099
C_1 - C_2 1.397
C_1 - H_2 1.087
C_1 - H_4 1.090
H_1 - C_2 - C_1 114.3
H_2 - C_1 - C_2 121.1
H_4 - C_1 - C_2 121.8

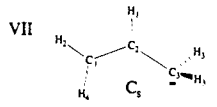

C_1 - C_2 1.352 C_1 - C_2 - C_3 125.2
C_3 - C_2 1.485 H_4 - C_1 - C_2 119.7
H_4 - C_1 1.088 H_2 - C_1 - C_2 121.9
H_2 - C_1 1.093 H_1 - C_2 - C_1 113.3
H_1 - C_2 1.114 H_3 - C_3 - C_2 111.0
H_3 - C_3 1.103 H_3 - C_3 - C_2 - C_1 119.8

Figure 2. Allyl anion structures obtained at the MP2/6-31+G(D) level of theory.

Allyl Anion

In the case of the parent anion, a preliminary exploration of the potential energy surface gave no indication that rotational isomerism involved anything but the perpendicular transition intermediate. It is not surprising that the allyl anion does not require any special C_1 distortions in order to stabilize the migration of negative charge to a terminal carbon. The important structural accommodation here is the pyramidalization of that terminal carbon associated with sp^3 hybridization that was not present in the allyl cation case.[15] We have, therefore, only considered stationary points corresponding to structures VI and VII. Energy

(10) Möller, C.; Plesset, M. S. *Phys. Rev.* **1934**, *46*, 618. Pople, J. A., Binkley, J. S.; Seeger, R. *Int. J. Quant. Chem.* **1976**, *10*, 1.
(11) Pople, J. A.; Head-Gordon, M.; Raghavachari, K. *J. Chem. Phys.* **1987**, *87*, 5968.
(12) Pople, J. A.; Head-Gordon, M.; Fox, D. J.; Raghavachari, K.; Curtiss, L. A. *J. Chem. Phys.* **1989**, *90*, 5622.
(13) Purvis, G. D.; Bartlett, R. J. *J. Chem. Phys.* **1982**, *76*, 1910. Paldus, J.; Cizek, J.; Shavitt, I. *Phys. Rev. A* **1972**, *5*, 50.
(14) Raghavachari, K.; Trucks, G. W.; Pople, J. A.; Head-Gordon, M. *Chem. Phys. Lett.* **1989**, *157*, 479.
(15) Carbanions of this type are normally found to be nonplanar: Hammons, J. H.; Hrovat, D. A.; Borden, W. T. *J. Phys. Org. Chem.* **1990**, *3*, 635. Gobbi, A.; MacDougall, P. J.; Frenking, G. *Angew. Chem., Int. Ed. Engl.* **1991**, *30*, 1001.

Table IV. 1,1,3,3-Tetramethylallyl Ions: Selected Geometric Parameters[a] and Energies

	cation **XIII** at 6-31G(D)			anion **XV** at 6-31+G(D)		
	RHF	MP2-FC	RHF-RF[b]	RHF	MP2-FC	RHF-RF[c]
H_1–C_2	1.074	1.087	1.074	1.086	1.101	1.086
C_2–C_3	1.387	1.396	1.387	1.392	1.405	1.392
C_3–C_5	1.493	1.485	1.493	1.511	1.509	1.511
H_1–C_2–C_3	115.5	115.6	115.5	111.5	112.7	111.5
C_2–C_3–C_5	118.1	118.2	118.1	118.3	116.6	118.3
C_2–C_3–C_7	126.8	125.9	126.8	124.8	122.3	124.8
C_3–C_5–H_9	113.2	113.5	113.2	111.8	111.4	111.8
H_1–C_2–C_3–C_5	2.169	1.275	2.146	17.88	18.91	17.88
C_5–C_2–C_3–C_7	−179.4	−179.8	−179.4	−204.6	−215.9	−204.6
C_2–C_3–C_5–H_9	7.138	3.219	6.993	−23.63	−31.01	−23.63
C_2–C_3–C_7–C_{15}	164.9	172.8	165.1	160.4	175.3	160.4
energy[d] (au)	−2.395145	−3.280268	−2.457677	−2.551384	−3.501595	−2.611172

[a] Distances in angstroms, angles in degrees. [b] Reaction field model with dielectric constant 78.5 and a spherical cavity radius of 4.18 Å. [c] Reaction field model with dielectric constant 78.5 and a spherical cavity radius of 4.37 Å. [d] Relative to −270 hartrees.

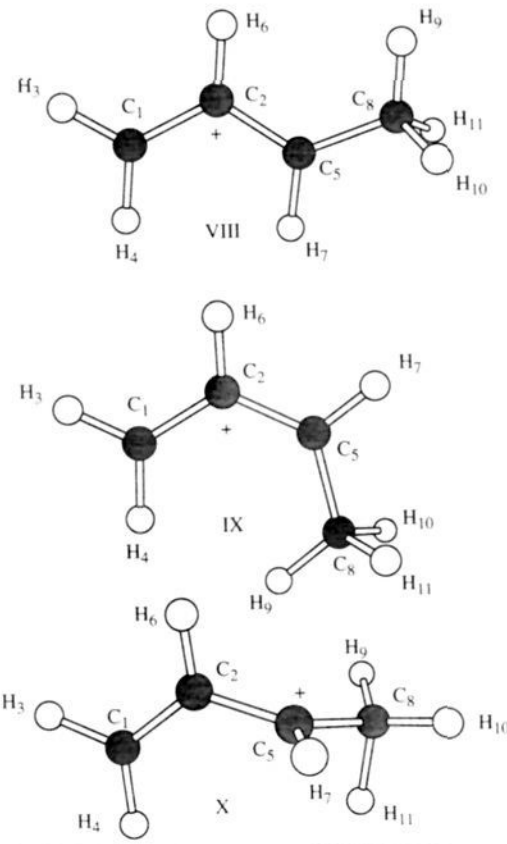

Figure 3. Methylallyl cation structures, MP2/6-31G(D).

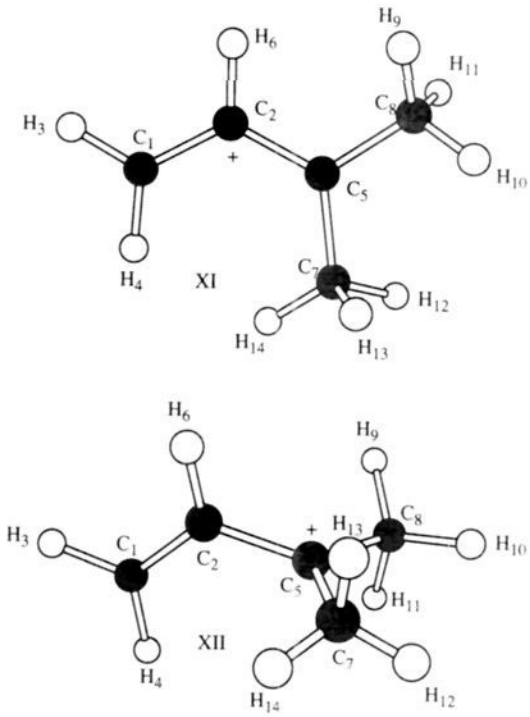

Figure 4. 1,1-Dimethylallyl cation structures, MP2/6-31G(D).

data are given in Table III. The MP2-Fu/6-31+G(D) optimized structures for the anion are given in Figure 2. Gas-phase geometries show little dependence on diffuse functions or electron correlation. Placement of this species in a medium of dielectric constant 78.5 also does little to change geometric parameters. This is to be expected, since the reaction field model used here is a spherical cavity within the dipole approximation, and the theoretical dipole moment of this structure is small. The spherical cavity radius, 3.60 Å, is the one recommended[16] on the basis of a calculation of molar volume.

Next, consider the rotational transition structure. Energy data are given in Table II, while Figure 2 shows the MP2/6-31+G(D) optimized structure. Inclusion of diffuse functions in the basis set increases the H_3–H_3–C_2 angle while decreasing the H_3–C_3–C_2–C_1 dihedral angle. A similar trend occurs when including electron correlation. Overall, the geometries are fairly unaffected by changes in the level of theory. For the solvated rotational transition structure, again little geometric change occurs, but an important energetic stabilization is made possible by the nontrivial dipole moment of this species. Calculated barriers to rotation for allyl anion are summarized in Table VI. Here the scaled RHF/6-31+G(D) zero-point vibrational energies have been included. For VI and VII these are 38.0 and 37.6 kcal/mol in the gas phase and 37.8 and 37.8 kcal/mol in solution. The gas-phase rotational barrier of 21 kcal/mol is calculated to be reduced to 17 kcal/mol in a medium of dielectric constant 78.5.

1,1,3,3-Tetramethylallyl Ions

The next question we wished to address was whether replacing the four hydrogens on the terminal carbons of allyl cation would offer any electronic stabilization of the type II stationary point. This is particularly relevant since the experimental work reported for rotational barriers had assumed this type of intermediate. Data for the equilibrium structure for 1,1,3,3-tetramethylallyl cation and anion are reported in Table IV. Definitions for atomic labels are given in Figures 5 and 6. The 6-31G(D) and 6-31+G(D) basis sets are used for the cation and anion, respectively, since little improvement was gained by extending these basis sets for the allyl cation case. Comparison of results from the parent cation shows that tetramethylation slightly increases the C–C bond length

(16) Wong, M. W.; Wiberg, K. B.; Frisch, M. J. *J. Chem. Phys.* **1991**, *95*, 8991.

Table V. 1,1,3,3-Tetramethylallyl Ions TS: Selected Geometric Parameters[a] and Energies

	cation **XIV** at 6-31G(D)			anion **XVI** at 6-31+G(D)		
	RHF	MP2-FC	RHF-RF[b]	RHF	MP2-FC	RHF-RF[c]
H_1–C_2	1.082	1.095	1.082	1.107	1.130	1.105
C_2–C_3	1.326	1.347	1.325	1.335	1.355	1.334
C_2–C_4	1.471	1.458	1.473	1.496	1.471	1.499
C_3–C_5	1.506	1.500	1.507	1.513	1.507	1.513
C_4–C_6	1.472	1.458	1.470	1.524	1.512	1.524
H_1–C_2–C_3	121.9	121.4	121.8	114.2	115.1	114.2
C_2–C_3–C_5	120.7	120.5	120.6	122.2	122.1	122.2
C_2–C_3–C_7	123.7	123.3	124.0	123.3	122.2	123.5
C_3–C_5–H_9	112.2	112.2	112.2	111.6	110.8	111.7
H_1–C_2–C_3–C_5	0.676	0.988	0.529	0.000	−0.005	0.000
H_1–C_2–C_4–C_6	82.02	82.51	81.81	58.33	58.95	58.25
C_5–C_2–C_3–C_7	180.5	180.5	180.5	180.0	180.0	180.0
C_6–C_2–C_4–C_8	−175.9	−177.2	−175.9	−116.7	−117.8	−116.5
C_2–C_3–C_5–C_9	1.493	1.998	1.252	−0.001	0.003	0.000
C_2–C_4–C_6–H_{10}	33.57	31.78	31.04	62.97	61.83	62.82
C_2–C_3–C_7–H_{15}	124.3	126.4	124.0	120.9	120.6	121.0
C_2–C_4–C_8–H_{17}	157.5	161.4	154.8	−183.0	−183.2	−182.9
energy (au)[d]	−2.361523	−3.242619	−2.426692	−2.537362	−3.485349	−2.599860

[a] Distances in angstroms, angles in degrees. [a] Distances in angstroms, angles in degrees. [b] Reaction field model with dielectric constant 78.5 and a spherical cavity radius of 4.19 Å. [c] Reaction field model with dielectric constant 78.5 and a spherical cavity radius of 4.40 Å. [d] Relative to −270 hartree.

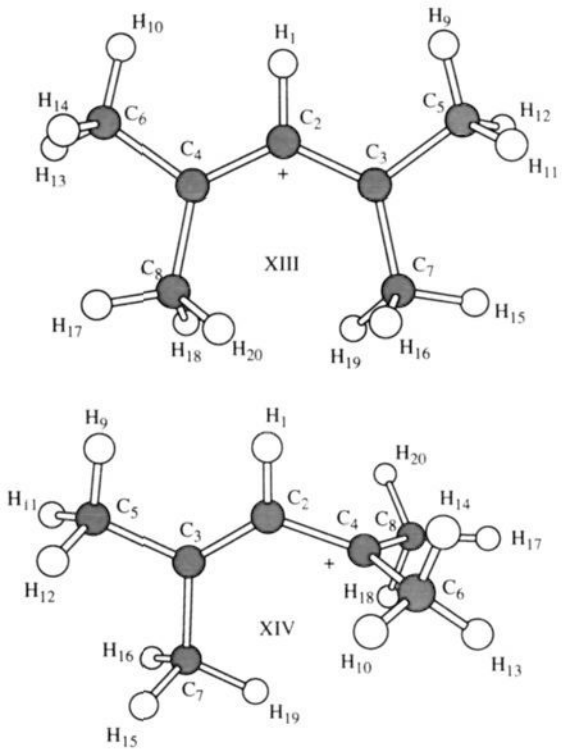

Figure 5. 1,1,3,3-Tetramethylallyl cation structures, MP2/6-31G(D).

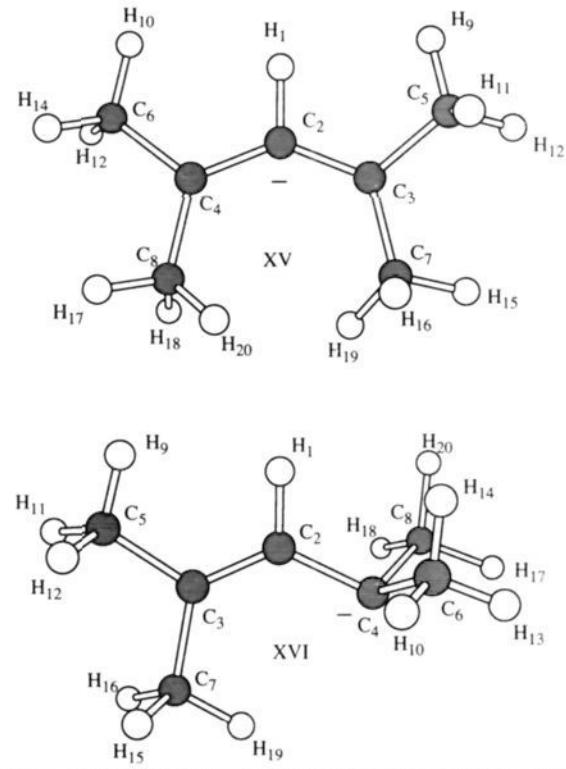

Figure 6. 1,1,3,3-Tetramethylallyl anion structures, MP2/6-31+G(D).

and reduces the H–C–C bond angle. For the anion, there is an even larger increase in the C–C bond length, making it somewhat comparable to the cation for the tetramethylallyl case. Electron correlation at the MP2 level does not affect results significantly for either the cation or the anion. Again, since the dipole moment is small, there is little structural change afforded by medium effects in either case.

Unlike the parent species, rotational transition structures of type II were found at the MP2 level for the 1,1,3,3-tetramethylallyl cation. Results are presented in Table V, and for the most part they are not significantly different from the HF geometric parameters. No significant geometric change is afforded by the reaction field.

In order to address the question of which methyl groups are actually important in reducing the complexity of isomerization in allyl cation, we attempted a series of MP2 geometry optimizations of the type II structure for various methyl-substituted species. With R_{2a} and R_{3a} being the only methyl groups, the perpendicular transition structure does not exist. If R_{2b} is the only methyl group or if both R_{2b} and R_{3b} are methyl groups, then the perpendicular transition structure does exist. Therefore, the essential element of the stabilization appears to be the donation of charge to the terminal carbon whose substituents are involved in the rotation. A single methyl group appears to be all that is needed to accomplish this.

Rotational Barriers and Atomic Charges

Table VI contains a summary of the data concerning the barrier to rotation in allyl ions which isomerize via the perpendicular transition structure. Here the RHF/6-31G(D) and the RHF/6-31+G(D) zero-point energies (both scaled by 1/1.12) have been included for the cation and anion, respectively. Consider first the gas-phase cation results. Using the barrier to proton migration in allyl cation, there is a decrease in the gas-phase isomerization

Table VI. Barrier to Rotation (kcal/mol) of Allyl Ions[a]

	dielectric constant	
	1.0	78.5
allyl anion		
RHF/6-31G(D)	20.0	
RHF/6-31+G(D)	20.8	17.3
MP2-FU/6-31+G(D)	20.9	
methylallyl cation		
RHF/6-31G(D)	24.3	
MP2-FC/6-31G(D)	25.2	
1,1-dimethylallyl cation		
RHF/6-31G(D)	15.2	
MP2-FC/6-31G(D)	15.6	
1,1,3,3-tetramethylallyl cation		
RHF/6-31G(D)	19.4	17.8
MP2-FC/6-31G(D)	21.9	
1,1,3,3-tetramethylallyl anion		
RHF/6-31G(D)	11.6	
RHF/6-31G(D)	8.6	7.0
MP2-FC/6-31+G(D)	10.0	

[a] The allyl cation is not included in this table since its "rotation" occurs via a different process.

barrier as methyl groups are positioned on the carbon involved in the rotation (5 kcal/mol for the first methyl, an additional 10 kcal/mol for the second. The first methyl leads, of course, to a change in mechanism and therefore gives a smaller effect than the second). The barrier is increased again when two additional methyl groups are positioned on the opposite terminal carbon (5 kcal/mol over the dimethylallyl case). This indicates that localization of positive charge in the perpendicular transition structure is best supported by the donation of electrons from locally positioned methyl groups. Donation of electrons from methyl groups on the opposite side delocalizes charge in allyl cation, resulting in a relative destabilization of the rotational transition structure.

It is often satisfying to discuss more quantitatively the relationship between features of a potential energy surface and populations of electrons at atomic centers. In the case of allyl cation, it would be desirable to correlate rotational barriers with changes in atomic populations or the migration of positive charge during the process. Many techniques have been proposed which allow the calculation of atomic charges from molecular wave functions. We have chosen to concentrate on two generally applicable methods: the natural population analysis (NPA)[17] and Bader's theory of atoms in molecules (AIM).[18] The results obtained using other methods of calculating charges are available as supplementary material. The best way to compare these techniques and to obtain useful information about the rotational barrier is to consider the charges on the groups and how they change during isomerization. Table VII lists results for the parent allyl cation and the dimethylallyl cation in both planar and rotated forms. The dimethyl case was chosen since it provides the most dramatic electronic effect on rotational barrier stabilization. Geometries are those optimized at the theoretical level listed (except for the MP2/6-31G(D) rotated parent compound, which was done at the RHF/6-31G(D) structure, since none was available from MP2 theory). The migration of charge on going from planar to rotated forms in the parent cation is about +0.2e using the AIM analysis and about +0.3e using the NPA method. In the dimethyl case, there is already a marked transfer of charge just from the methylation of the planar parent cation. Isomerization of the dimethylallyl cation then requires only 0.1e to migrate according to AIM analysis or 0.2e using the NPA. This is consistent with the calculated rotational barriers.

Two features of the calculated charge distributions are worth noting. First, there is a significant change in population on going from RHF to MP2 wave functions. The changes are enough to reverse the sign of the charge at the center CH group of allyl cation in several cases, and they led to a net decrease in electron population of about 0.1e. These changes are larger than we have observed previously with neutral compounds.[19]

Table VII. Charges of the Groups in $CH_2CHCR_2^+$ Cations[a]

	HF/6-31G*		MP2/6-31G*	
group	NPA	AIM	NPA	AIM
		Planar R = H		
CH_2	0.586	0.347	0.523	0.389
CH	−0.173	0.308	−0.046	0.222
		Rotated R = H		
CH_2^+	0.912	0.478	0.874	0.560
CH	−0.172	0.108	−0.104	0.080
CH_2	0.260	0.414	0.230	0.360
		Planar R = CH_3		
CMe_2	0.709	0.532	0.648	0.692[b]
CH	−0.170	0.206	−0.048	0.138
CH_2	0.461	0.262	0.400	0.170[b]
		Rotated R = CH_3		
CMe_2	0.910	0.661	0.885	0.722
CH	−0.108	0.042	−0.058	0.050
CH_2	0.198	0.297	0.173	0.228

[a] NPA = natural population analysis; AIM = atoms in molecules. The group charges were obtained by summing the charges associated with the atoms in each group. [b] Difficulty was found with the integration of two hydrogens. They were assumed to have equal charges, and as a result the integrals may have an error of ~0.01e.

Second, the sign of the charge at the center CH group might be noted. In allyl cation, the electron-deficient terminal methylene groups would be expected to inductively remove charge from the central CH. In another study, we have found that the loss of an electron from allyl radical to form the cation involves a decrease in electron population at all groups,[20] supporting the contention that the central CH should have a positive charge. The AIM populations lead to the expected charge, but the natural population analysis gives a group with a negative charge even with MP2 wave functions. With the dimethylallyl cation, the central CH has a negative charge with the NPA populations, but has the expected positive sign with the AIM populations. The charges calculated by the various methods need further study, and we are in the process of gathering the needed data for a variety of organic and inorganic compounds.[21]

Conclusions

A surprising result has been afforded from the gas-phase study of the parent allyl cation. Using levels of theory which include electron correlation (beyond HF), we were unable to locate a C_s stationary point corresponding to the perpendicular rotational transition structure. Instead, the multistep process described above is preferred. Methylation of the parent cation stabilizes the more traditional transition structure. Trends in the rotational barrier due to methyl substitution can be effectively rationalized in terms of changes in the charge on the rotating unit. Various methods, including potential-derived charges and natural bond analysis, provide similar absolute magnitudes for this charge. AIM analysis leads to slightly lower absolute charges. All techniques lead to the same conclusions based on relative changes in group charge during isomerization. Finally, solvation effects on the isomerization process have been calculated to be much smaller than the effect of methyl substitution. For a medium of dielectric constant 78.5, the barriers are reduced by only 2–3 kcal/mol. This amount does, however, bring the 1,1,3,3-tetramethylallyl cation barrier into the

(17) Reed, A. E.; Curtiss, L. A.; Weinhold, F. *Chem. Rev.* **1988**, *88*, 899. Carpenter, J. E.; Weinhold, F. *J. Mol. Struct.* **1988**, *169*, 41.
(18) Bader, R. F. W. *Atoms in Molecules: A Quantum Theory*; Clarendon Press: Oxford, 1990.
(19) Wiberg, K. B.; Hadad, C. M.; LePage, T. J.; Breneman, C. M.; Frisch, M. J. *J. Phys. Chem.* **1992**, *96*, 671. Wiberg, K. B.; Hadad, C. M.; Rablen, P. R.; Cioslowski, J. *J. Am. Chem. Soc.* **1992**, *114*, 8644.
(20) Wiberg, K. B.; Schleyer, P. v. R. Manuscript in preparation.
(21) Wiberg, K. B.; Rablen, P. R. Manuscript in preparation.

range of the experimental estimate.

Calculational Details

All of the calculations described in this work were performed using the Gaussian suite of programs[22] running on a Multiflow Trace-14/300 and a Silicon Graphics 4D/320 workstation. Geometry optimizations were greatly facilitated by its ability to calculate analytic first derivatives for the HF, MP2, and QCISD methods as well as analytic second derivatives for the HF[23] and MP2[24] methods. The AIM charges were calculated using PROAIM.[25]

Acknowledgment. This work was supported by a grant from the National Institutes of Health and by Lorentzian Inc.

Supplementary Material Available: Full lists of geometric parameters for all optimizations performed (9 pages). Ordering information is given on any current masthead page.

(22) Gaussian 92, revision A: Frisch, M. J.; Trucks, G. W.; Head-Gordon, M.; Gill, P. M. W.; Wong, M. W.; Foresman, J. B.; Johnson, B. G.; Schlegel, H. B.; Robb, M. A.; Replogle, E. S.; Gomperts, R.; Andres, J. L.; Raghavachari, K.; Binkley, J. S.; Bonzalez, C.; Martin, R. L.; Fox, D. J.; Defrees, D. J.; Baker, J.; Stewart, J. J. P.; Pople, J. A. Gaussian, Inc., Pittsburgh, PA, 1992.

(23) Pople, J. A.; Krishnan, R.; Schlegel, H. B.; Binkley, J. S. *Int. J. Quant. Chem. Symp.* **1979**, *13*, 225. Frisch, M. J.; Head-Gordon, M.; Pople, J. A. *Chem. Phys.* **1990**, *141*, 189.

(24) Trucks, G. W.; Frisch, M. J.; Head-Gordon, M.; Andres, J. L.; Schlegel, H. B.; Salter, E. A. *J. Chem. Phys.*, in press.

(25) Biegler-König, F. W.; Bader, R. F. W.; Tang, T.-H. *J. Comput. Chem.* **1982**, *3*, 317.

Theoretical Study of the Inversion of the Alcohol Acidity Scale in Aqueous Solution. Toward an Interpretation of the Acid-Base Behavior of Organic Compounds in Solution

Iñaki Tuñón, Estanislao Silla,* and Juan-Luis Pascual-Ahuir

Contribution from the Departamento de Química-Física, Universidad de Valencia, 46100 Burjasot, Valencia, Spain. *Received August 17, 1992*

Abstract: Some homologous series of organic compounds present an acid-base behavior in solution very different from that in the gas phase. The series formed by MeOH to *t*-BuOH is a representative example of these series with a gas-phase acidity order (*t*-BuOH > *i*-PrOH > EtOH > MeOH) following the greater ability of the methyl group relative to hydrogen to stabilize the charged centers while in solution the final ordering is just the opposite. In this paper, the change in the alcohol's acidity scale when passing from the gas phase to solution is studied. Gas-phase energies are calculated at the MP4 level with the 6-31G* basis set and an sp diffuse function added on the oxygen atom. Calculated deprotonation free energies are in very good agreement with the experimental values. Solvation energies are obtained in the framework of the continuum model using a quantum description of the solute charge distribution. The main contribution to the change in the acidity scale in solution is the electrostatic component of the solvation energy of the basic forms, and the charge delocalization produced by the progressive substitution of hydrogen atoms by methyl groups can be used to understand the order in solution. Our results, which reproduce quite well experimental ordering and magnitude, seem to indicate that a simple electrostatic argument could explain the origin of this inversion and can be employed to rationalize the acid-base behavior of some homologous series.

Introduction

The development of several techniques such as high-pressure mass spectrometry[1] and flowing afterglow[2] and ion cyclotron resonance (ICR) spectrometry[3] has provided an accurate set of thermochemical data for acidities and basicities of organic compounds in the gas phase.[4] From the acidity-basicity order of some homologous series in the gas phase (NH_3 to Me_3N and MeOH to *t*-BuOH) it became clear that simple charge-induced dipole interaction models could explain the effect of increased charge-releasing ability of the methyl group compared with hydrogen.[5,6] However, in solution these same series present an irregular order or just the opposite[6] order from that in the gas phase. This different behavior is a good test for theories and models to estimate the solvation free energies and molecular properties in solution. Calculation and understanding of acidity-basicity free energies in solution are some of the most important challenges for theoretical methods because they are the key to interpreting several reaction mechanisms in solution.[7] In a recent work[8] we have dealt with the irregular ordering of methylamines' basicities by using the polarizable continuum model of the solvent,[9] obtaining a good agreement with experimental data. Moreover it was shown that the methyl substitution, while stabilizing charged species in vacuo, diminishes the energies of interaction with the solvent. These two opposite trends result in an irregular basicity ordering in solution for methylamines.

The alcohols present a homologous series for which a total inversion in the acidity scale is produced when going from the gas phase to solution. This series is formed by MeOH to *t*-BuOH. The gas-phase acidity ordering is *t*-BuOH > *i*-PrOH > EtOH > MeOH, following the greater ability of the methyl group relative

(1) (a) Yamdagni, R.; Kebarle, P. *J. Am. Chem. Soc.* **1978**, *100*, 1320. (b) Kebarle, P. *Ann. Rev. Phys. Chem.* **1977**, *28*, 445.

(2) Bohme, D. K. In *Interactions Between Ions and Molecules*; Ausloos, P., Ed.; Plenum Press: New York, 1974; p 489.

(3) Wolf, J. F.; Staley, R. H.; Koppel, I.; Taagepera, M.; McIver, R. T., Jr.; Beauchamp, J. L.; Taft, R. W. *J. Am. Chem. Soc.* **1977**, *99*, 5417.

(4) Bartmess, J. E.; Scott, J. A.; McIver, R. T., Jr. *J. Am. Chem. Soc.* **1979**, *101*, 6046.

(5) Aue, D. H.; Webb, H. M.; Bowers, M. T. *J. Am. Chem. Soc.* **1976**, *98*, 318.

(6) Aue, D. H.; Webb, H. M.; Bowers, M. T. *J. Am. Chem. Soc.* **1976**, *98*, 311.

(7) Lim, C.; Bashford, D.; Karplus, M. *J. Phys. Chem.* **1991**, *95*, 5610.

(8) (a) Pascual-Ahuir, J. L.; Andrés, J.; Silla, E. *Chem. Phys. Lett.* **1990**, *169*, 297. (b) Tuñón, I.; Silla, E.; Tomasi, J. *J. Phys. Chem.* **1992**, *96*, 9043.

(9) (a) Miertus, S.; Scrocco, E.; Tomasi, J. *Chem. Phys.* **1981**, *55*, 117. (b) Bonaccorsi, R.; Cimiraglia, R.; Tomasi, J. *J. Comput. Chem.* **1983**, *4*, 567.

0002-7863/93/1515-2226$04.00/0